Optics Communications 285 (2012) 5128–5131

Contents lists available at SciVerse ScienceDirect

Optics Communications

journal homepage: www.elsevier.com/locate/optcom

Intensity curvature sensor based on photonic crystal fiber with three coupled cores

H. Martins [a,b,*], Manuel B. Marques [a,b], Pedro Jorge [a], Cristiano M.B. Cordeiro [c], Orlando Frazão [a]

[a] INESC TEC (formerly INESC Porto), Rua do Campo Alegre 687, 4169-007 Porto, Portugal
[b] Faculdade de Ciências da Universidade do Porto, Rua do Campo Alegre 687, 4169-007 Porto, Portugal
[c] Instituto de Física "Gleb Wataghin," Universidade Estadual de Campinas—UNICAMP, Campinas, São Paulo, Brazil

ARTICLE INFO

Article history:
Received 1 February 2012
Received in revised form
26 July 2012
Accepted 27 July 2012
Available online 14 August 2012

Keywords:
Photonic crystal fiber
Optical fiber sensor
Intensity curvature sensor

ABSTRACT

An intensity curvature sensor using a Photonic Crystal Fiber (PCF) with three coupled cores is proposed. The three cores were aligned and there was an air hole between each two consecutive cores. The fiber had a low air filling fraction, which means that the cores remain coupled in the wavelength region studied. Due to this coupling, interference is obtained in the fiber output even if just a single core is illuminated. A configuration using reflection interrogation, which used a section fiber with 0.13 m as the sensing head, was characterized for curvature sensing. When the fiber is bended along the plane of the cores, one of the lateral cores will be stretched and the other compressed. This changes the coupling coefficient between the three cores, changing the output optical power intensity. The sensitivity of the sensing head was strongly dependent on the direction of bending, having its maximum when the bending direction was along the plane of the cores. A maximum curvature sensitivity of 2.0 dB/m^{-1} was demonstrated between 0 m and 2.8 m.

1. Introduction

In recent years, PCFs have been widely used both in research and industry. Recent reports have demonstrated the possibility of using multicore PCFs for several applications, such as light couplers [1–4], narrow band filters [5,6], frequency comb generators based on four-wave mixing [7], supercontinuum generation [8], phase-locking [9] and fiber lasers [10].

Experimental studies comparing the properties of light in a PCF for a number of cores up to eighteen for high power applications have been presented [11]. Theoretical models have also been presented to describe the supermode characteristics for linearly and circularly distributed multicores in PCFs [12] and the dependence of the characteristics of these modes on the geometry of the fiber [13]. PCFs have also been used for sensing applications [14], such as biomolecules [15], force meters [16], pressure [17], torsion [18], strain [19], temperature [20] and curvature sensors [21].

In curvature sensors, three measurands can be used to interrogate the sensor, namely, the phase shift [21], bending losses [22] or wavelength separation [23]. With the use of FBGs written into separate cores of multicore PCFs, sensors with temperature insensitivity for one-axis [23] and two-axis [24] curvature measurement have been demonstrated. The sensors make use of the different strain applied in different cores when curvature is applied to the fiber to induce different shifts in the wavelengths of the FBGs. The same principle has also been demonstrated in Gemini fibers [25].

An intensity curvature sensor was demonstrated to measure curvature with a sensitivity of 2.16 ± 0.02 dB/m^{-1} in a range of 3.5 m^{-1} using long-period fiber grating monitored by an optical time-domain reflectometer [26]. For shorter measuring ranges, higher sensitivities have been achieved. Using a fiber-optic curvature sensor based on the single-mode-multimode-single-mode (SMS) fiber structure, a sensitivity of -18.42 dB/m^{-1} in a range of 0.54 m and a sensitivity of -130.37 dB/m^{-1} for a range of 0.23 m^{-1} was demonstrated [27].

In this paper, the authors present an intensity curvature sensor interrogated in reflection which uses a section of silica photonic crystal fiber with three aligned cores as the sensing element. This new configuration explores the variation of the coupling coefficient between the fiber cores when curvature is applied. The advantage of this sensing head is the simple interrogation technique based on optical power variation. The sensor was characterized for three different planes of curvature with respect to the cores alignment.

2. Experimental setup

Fig. 1 presents the configuration of the curvature sensor. The configuration uses a broadband source at 1550 nm with 100 nm

* Corresponding author at: INESC TEC (formerly INESC Porto), Rua do Campo Alegre 687, 4169-007 Porto, Portugal. Tel.: +351 916897310.
E-mail address: hfm@inescporto.pt (H. Martins).

0030-4018/$ - see front matter
http://dx.doi.org/10.1016/j.optcom.2012.07.074

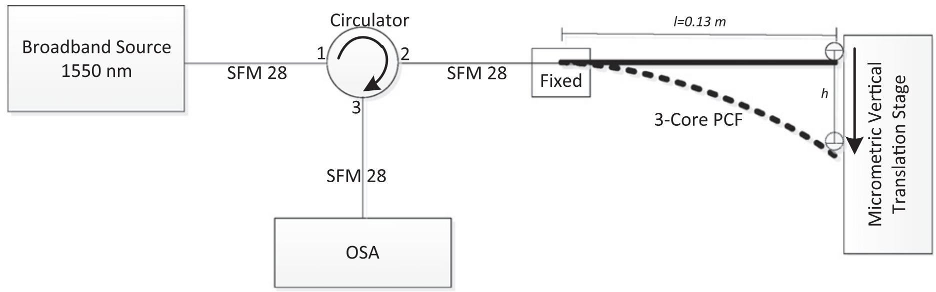

Fig. 1. Experimental setup of the bending sensor.

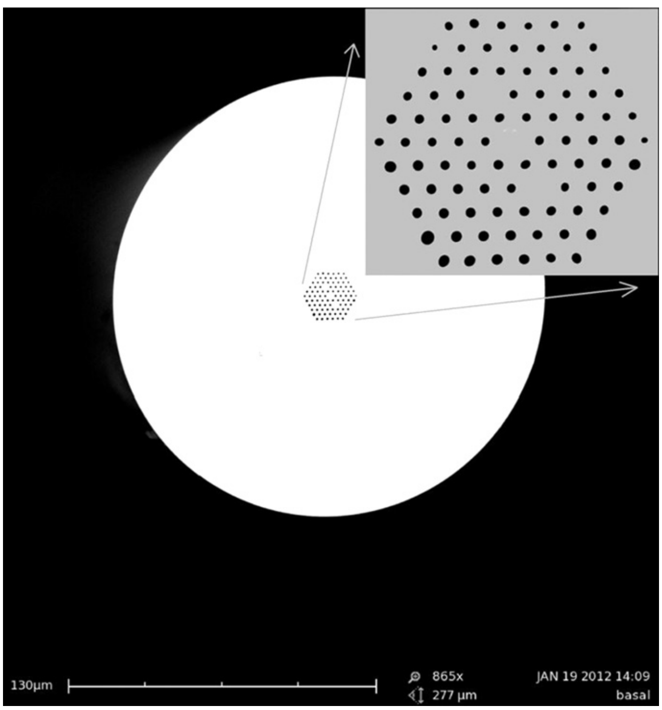

Fig. 2. Cross section of the PCF with three cores with a magnification of 865 × (inset figure with a magnification of 9000 ×).

bandwidth and an Optical Spectrum Analyzer (OSA), with a maximum resolution of 0.05 nm, which was used to observe the output optical spectrum. A photonic crystal fiber (PCF) with 0.13 m three aligned cores and a low air filling fraction is used as the sensing element. The average pitch of the air hole (Λ) of the fiber, i.e. the distance between two consecutive holes, was (2.17 ± 0.02) µm, the average diameter of the air holes (d) was (0.9 ± 0.1) µm and the fiber had a total of 88 air holes (N_{AH}). The relative hole diameter d/Λ was 0.41 ± 0.05 and the parameter λ/Λ was 0.71 ± 0.02 (considering a bandwidth of 100 nm). The diameter of the guiding cores was (3.6 ± 0.1) µm, the size of the air hole cladding structure was (22.5 ± 0.1) µm and the diameter of the cladding was 184 µm. A transversal cross-area section of the PCF geometry is presented in Fig. 2. One end of the PCF is spliced with the SMF 28 and the other end is free. The core of the SMF is aligned with the central core of the PCF so that the coupling between the SMF and the side cores of the PCF is low. In order to enable real applications using PCF it is essential to have low loss splices with standard single-mode fibers. Although the different coefficients of thermal expansion and melting temperatures of the two fibers makes the splicing difficult, low-loss splices have been demonstrated between SMF 28 and PCFs fibers [28].

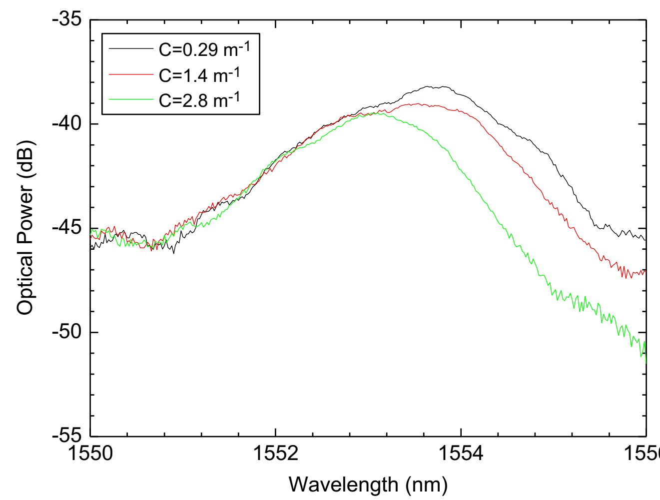

Fig. 3. Spectral response for different applied curvature (reflection setup).

The light sent by the light source is reflected in the cleaved free end of the PCF by Fresnel reflection (4%) and is deflected in the circulator to the OSA. In this case, the output signal is observed in reflection and the effective optical path in the PCF is twice its physical length. The curvature of the PCF is applied by vertically moving the micrometric translation stage. A good approximation for the curvature C is given by

$$C = \frac{1}{R} = \left(\frac{2h}{l^2 + h^2}\right), \tag{1}$$

where R is the curvature radius h is the height difference between the fixed end and the free end of the PCF and l is the horizontal distance between the fixed end of the PCF and the micrometric translation stage.

3. Results

Using the setup described in Fig. 1, curvature was applied to the PCF. The spectral response of the peak which presented the highest stability and optical power of the output spectrum for different applied curvature is presented in Fig. 3. Although the form of the spectrum remains similar the average optical power decreases for higher applied curvature.

The average optical power (per nm) between 1550 nm and 1556 nm (the range which was correspondent to the peak presented in Fig. 3 and which presented the highest sensitivity of the output spectrum) was measured as a function of the curvature (Fig. 4) when the bending direction had an angle with the plane of the cores of 0 degrees (along the plane of the cores), 30 degrees and 90 degrees (perpendicular to the plane of the cores).

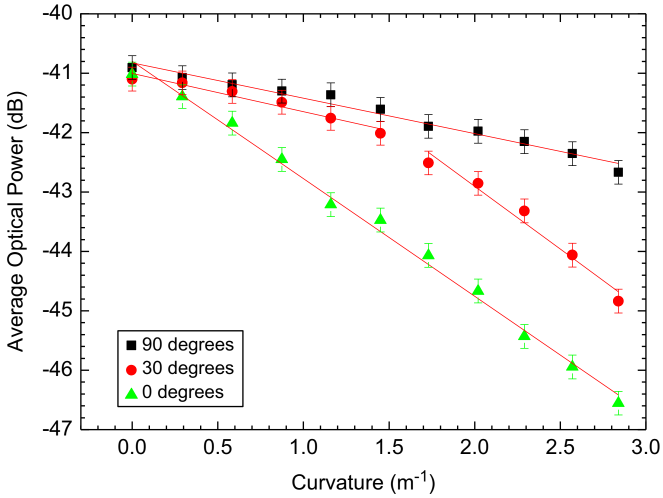

Fig. 4. Average optical power vs. curvature for rotation angles of 0°, 30° and 90° of the PCF along its axis (solid lines are a linear fit of the experimental data; for the 30 degrees measurements two regimes are considered: low curvatures (0–1.5 m^{-1}) and high curvatures (1.7–2.8 m^{-1})).

When the fiber is bended, the coupling coefficient between the three cores is changed. If the fiber is bended along the plane of the cores, one of the lateral cores will be stretched and the other compressed, inducing a high variation of the coupling coefficient. In this case, high sensitivity is expected due to the exchange of optical power between the lateral cores and the central core. However, if the bending direction is perpendicular to the plane of the cores, the lateral cores will experience a similar mechanical stress, resulting in a small variation of the coupling coefficient. In this case, when the curvature is applied, optical power is lost to the cladding. Therefore, the coupling coefficient (and the curvature sensitivity) will strongly depend on the direction of bending, having its maximum when the bending direction is along the plane of the cores and its minimum when the bending direction is perpendicular to the plane of the cores.

The side cores are weakly coupled to the SMF and therefore the optical power transferred from the PCF to the SMF will be mostly the optical power in the central core. Since the optical power transferred from the central core to the side cores is dependent on the coupling coefficient between the cores, the output optical power will be dependent on the coupling coefficient, which in turn is dependent on the curvature.

A theoretical model is being developed in which the dependence of the coupling coefficient between the three cores in the curvature and the other parameters of the fiber will be explicitly given. However, the coupling coefficient should be dependent on the diameter of the air holes (mainly the ones between the cores) d and the diameter of the cores. Furthermore, although the V-parameter was not calculated, the values of the relative hole diameter d/Λ, the parameter λ/Λ and diameter of the cores place the fiber in the "single-mode" operation region (each core should only have one mode when considered separately) [29].

The main results are resumed in Table 1. As expected, the sensitivity of the average optical power with the curvature was higher when the bending direction was along the plane of the cores (0 degrees). With a rotation angle of 0 degrees, a linear response with a curvature sensitivity of 2.0 ± 0.1 dB/m^{-1} was obtained. As for the angle of 90 degrees, linear response with a curvature sensitivity of 0.60 ± 0.06 dB/m^{-1} was also obtained, i.e. approximately three times lower than the 0 degrees measurement.

Regarding the measurement with an angle of 30 degrees (between the two previous angles) a non-linear behavior was observed. This behavior is the combination of the two effects explained previously, i.e., for low curvatures, the behavior is similar to the 90 degrees case since the optical power exchange between the cores is not strong. However, for high curvatures, the optical power exchange between central and lateral cores will be higher and a behavior similar to the 0 degrees case is observed. Furthermore, optical power will be lost to the cladding, providing an even higher sensitivity than the 0 degrees measurement. The non-linear response was divided in two linear regimes, for low curvatures and high curvatures. For the low curvatures regime (0–1.5 m^{-1}), a sensitivity of 0.6 ± 0.1 dB/m^{-1} was achieved and for the high curvatures regime (1.7–2.8 m^{-1}), a sensitivity of 2.1 ± 0.4 dB/m^{-1} was obtained.

Table 1
Curvature sensor parameters.

	90 Degrees	30 Degrees		0 Degrees
Maximum average power variation (dB)	1.8 ± 0.4	3.7 ± 0.4		5.2 ± 0.4
Measurement range (m^{-1})	0–2.8	0–1.5	1.7–2.8	0–2.8
Curvature sensitivity (dB/m^{-1})	-0.60 ± 0.06	-0.6 ± 0.1	-2.1 ± 0.4	-2.0 ± 0.1

4. Conclusion

A new type of intensity curvature sensor using a three core PCF is demonstrated and characterized. The sensor makes use of the variation of the coupling coefficient between the fiber cores with curvature and was interrogated in optical power variation when the sensing head was subjected to curvature. Furthermore, the sensitivity can be tuned by applying the curvature along different planes. A maximum curvature sensitivity of 2.0 ± 0.1 dB/m^{-1} was obtained for a measurement range of 0–2.8 m^{-1}.

Although for shorter measurement ranges, sensors with much higher sensitivities sensor have been demonstrated [27], the presented sensor has a similar sensitivity than other fiber based intensity curvature sensors for similar measurement ranges [26]. Using interferometric techniques, curvature sensors with a sensitivity up to an order of magnitude higher than the presented sensor have been reported [23,30]. This sensor however is focused on providing a simpler interrogation scheme and also has the advantage of using a reflection interrogation scheme which is simpler to implement in practical applications. Furthermore, the sensitivity of the presented sensor can be increased while maintaining the simplicity of the interrogation scheme by increasing the length of the PCF.

Acknowledgments

H. Martins acknowledges a scholarship from FCT—Fundação para a Ciência e a Tecnologia (Portuguese Foundation for Science and Technology), SFRH/BD/76991/2011.

This work was supported by ANEEL through the research and development program of the companies of the group TBE—Transmissoras Brasileiras de Energia (EATE—Empresa Amazonense de Transmissão de Energia, ECTE—Empresa Catarinense de Transmissão de Energia, ENTE—Empresa Norte de Transmissão de Energia, ERTE—Empresa Regional de Transmissão de Energia, ETEP—Empresa Paraense de Transmissão de Energia, LUMITRANS—Companhia Transmissora de Energia Electrica and STC—Sistemas de Transmissão Catarinense), ERDF—European Regional Development

Fund through the COMPETE Programme (operational program for competitiveness) and by National Funds through the FCT—Fundação para a Ciência e a Tecnologia (Portuguese Foundation for Science and Technology) within Project FCOMP 01-0124-FEDER-022701.

References

[1] S.K. Varshney, K. Saitoh, R.K. Sinha, M. Koshiba, Journal of Lightwave Technology 27 (2009) 2062.
[2] Y. Yue, G.Y. Kai, Z. Wang, C.S. Zhang, Y.F. Lu, Y. Li, T.T. Sun, L. Jin, J.G. Liu, Y.G. Liu, S.Z. Yuan, X.Y. Dong, IEEE Photonics Technology Letters 18 (2006) 2032.
[3] J. Laegsgaard, O. Bang, A. Bjarklev, Optics Letters 29 (2004) 2473.
[4] M.Y. Chen, X.X. Fu, Y.K. Zhang, Journal of Physics D—Applied Physics 44 (2011) 405104.
[5] K. Saitoh, N.J. Florous, S.K. Varshney, M. Koshiba, Journal of Lightwave Technology 26 (2008) 663.
[6] K. Saitoh, N.J. Florous, M. Koshiba, M. Skorobogatiy, Optics Express 13 (2005) 10327.
[7] A.V. Husakou, J. Herrmann, Applied Physics Letters 83 (2003) 3867.
[8] J.M. Dudley, G. Genty, S. Coen, Review of Modern Physics 78 (2006) 1135.
[9] A. Mafi, J.V. Moloney, Journal of the Optical Society of America B—Optical Physics 21 (2004) 897.
[10] L. Michaille, D.M. Taylor, C.R. Bennett, T.J. Shepherd, B.G. Ward, Optics Letters 33 (2008) 71.
[11] L. Michaille, C.R. Bennett, D.M. Taylor, T.J. Shepherd, IEEE Journal of Selected Topics in Quantum Electronics 15 (2009) 328.
[12] C.Y. Guan, L.B. Yuan, J.H. Shi, Optics Communications 283 (2010) 2686.
[13] C.C. Wang, F. Zhang, R. Geng, C. Liu, T.G. Ning, Z. Tong, S.S. Jian, Optics Communications 281 (2008) 5364.
[14] G.A. Cardenas-Sevilla, V. Finazzi, J. Villatoro, V. Pruneri, Optics Express 19 (2011) 7596.
[15] J.B. Jensen, L.H. Pedersen, P.E. Hoiby, L.B. Nielsen, T.P. Hansen, J.R. Folkenberg, J. Riishede, D. Noordegraaf, K. Nielsen, A. Carlsen, A. Bjarklev, Optics Letters 29 (2004) 1974.
[16] M. Reimlinger, A. Colalillo, J. Coompson, R. Wynne, Proceedings of the Sensors and Smart Structures Technologies for Civil, Mechanical, and Aerospace Systems 2011, vol. 7981, 2011.
[17] D. Chen, G. Hu, L. Chen, IEEE Photonics Technology Letters 23 (2011) 1851.
[18] W.G. Chen, S.Q. Lou, L.W. Wang, H. Zou, W.L. Lu, S.S. Jian, IEEE Photonics Technology Letters 23 (2011) 1639.
[19] M. Deng, C.P. Tang, T. Zhu, Y.J. Rao, IEEE Photonics Technology Letters 23 (2011) 700.
[20] S.M. Nalawade, H.V. Thakur, IEEE Photonics Technology Letters 23 (2011) 1600.
[21] W.N. MacPherson, M.J. Gander, R. McBride, J.D.C. Jones, P.M. Blanchard, J.G. Burnett, A.H. Greenaway, B. Mangan, T.A. Birks, J.C. Knight, P.S. Russell, Optics Communications 193 (2001) 97.
[22] L. Michaille, D.M. Taylor, C.R. Bennett, T.J. Shepherd, C. Jacobsen, T.P. Hansen, Integrated Optical Devices, Nanostructures, and Displays 5618 (2004) 30.
[23] J.G. Burnett, P.M. Blanchard, A.H. Greenaway, Strain 36 (2000) 127.
[24] G.M.H. Flockhart, W.N. MacPherson, J.S. Barton, J.D.C. Jones, L. Zhang, I. Bennion, Optics Letters 28 (2003) 387.
[25] E. Zetterlund, A. Loriette, C. Sterner, M. Eriksson, H. Eriksson-Quist, W. Margulis, Journal of Sensors 2009 (2009) 196380.
[26] O. Frazao, R. Falate, J.M. Baptista, J.L. Fabris, J.L. Santos, Optical Engineering 44 (2005) 110502.
[27] Y. Gong, T. Zhao, Y.J. Rao, Y. Wu, IEEE Photonics Technology Letters 23 (2011) 679.
[28] O. Frazao, J.P. Carvalho, H.M. Salgado, Microwave and Optical Technology Letters 46 (2005) 172.
[29] B.T. Kuhlmey, R.C. McPhedran, C.M. de Sterke, P.A. Robinson, G. Renversez, D. Maystre, Optics Express 10 (2002) 1285.
[30] M.J. Gander, D. Macrae, E.A.C. Galliot, R. McBride, J.D.C. Jones, P.M. Blanchard, J.G. Burnett, A.H. Greenaway, M.N. Inci, Optics Communications 182 (2000) 115.